

ELEVENTH EUROPEAN ROTORCRAFT FORUM

Paper No. 95

IN-FLIGHT MEASUREMENT OF ROTOR HUB DRAG USING THE
RSRA--A FEASIBILITY DEMONSTRATION

C. W. Acree, Jr. and Robert M. Kufeld

Ames Research Center
Moffett Field, California, U.S.A.

September 10-13, 1985

London, England

THE CITY UNIVERSITY, LONDON, EC1V OHB, ENGLAND

IN-FLIGHT MEASUREMENT OF ROTOR HUB DRAG USING THE
RSRA--A FEASIBILITY DEMONSTRATION

C. W. Acree, Jr. and Robert M. Kufeld
Ames Research Center
Moffett Field, California, U.S.A.

ABSTRACT

The Rotor Systems Research Aircraft (RSRA) is a compound helicopter that was test flown as a fixed-wing aircraft, with the main rotor blades removed and the rotor hub installed. An onboard rotor load-measurement system measured the resulting rotor hub drag and lift. Measured hub drag and lift are plotted for comparison to that predicted by full-scale and 1/6-scale model wind tunnel tests. The success of the demonstration gives confidence that planned improvements to the RSRA will allow high-accuracy hub drag and lift measurements to be made in flight on a routine research basis.

1. INTRODUCTION

Reduction of helicopter parasite drag, including rotor hub drag, is a major objective in the quest for higher speed and efficiency. As helicopter speeds increase, reduction of drag becomes more important. To support research and design efforts, precise measurement of individual drag components also becomes increasingly desirable. Drag from the main rotor hub alone may contribute from 20% to 33% of the total drag (ref. 1). The Rotor Systems Research Aircraft (RSRA) has the capability of directly measuring hub drag in flight, independently of other drag components. This drag-measurement capability, consequently, makes this aircraft a valuable tool for validating design predictions and wind tunnel measurements of hub drag.

The RSRA is a compound (winged) helicopter built for NASA and the U.S. Army by Sikorsky Aircraft. It has a variable-incidence wing, two auxiliary propulsion engines, and a full set of fixed-wing controls. These features give it the unique ability to fly as a fixed-wing aircraft while carrying a full-size helicopter rotor system. It can also fly without any main rotor at all. It was so flown by NASA in the summer of 1984 at the NASA Ames-Dryden Flight Research Facility (refs. 2 and 3). By leaving the main-rotor hub installed without blades (as shown in fig. 1), experiments were performed to measure actual hub drag and lift in flight. The RSRA was also flown with the hub removed in order to acquire zero-drag reference data. (The compound RSRA should not be confused with the pure helicopter version of the RSRA, now undergoing conversion to the X-Wing testbed.)

The RSRA has several built-in load-measurement systems (fig. 2). The main-rotor load-measurement system is of interest here; it provides simultaneous, independent measurements of all forces and moments transmitted by the rotor to the airframe (ref. 4). Removal of the main-rotor blades or hub does not affect its operation. Therefore, the RSRA can directly measure the drag and lift of any rotor hub mounted to the main-rotor shaft.

Wind tunnel tests were run for a 1/6-scale model of the RSRA (ref. 5), and for full-scale models of rotor hubs (ref. 6) similar to the type installed on the RSRA during the fixed-wing flight tests. The flight tests allowed comparison of actual hub drag and lift to that predicted by the wind tunnel tests.

This particular experimental program was intended to be a feasibility demonstration, and not a fully refined drag survey. Its success gives confidence that experimental procedures are developed sufficiently to permit routine measurements of hub drag and lift by the RSRA, and that various proposed improvements to the aircraft are worth pursuing.

A special report was prepared by the American Helicopter Society on the general topic of helicopter parasite drag (ref. 7). Some of the articles referred to in the present paper are included in that report. Others (refs. 6, 10, 13, 14, and 15) are separate studies of the hub drag problem. A major wind tunnel test of the RSRA, including hub drag measurements, is reported in reference 5. The present paper will touch only briefly on a few of the many aspects of the problem of hub drag as an introduction to the RSRA test program. The reader may wish to consult the other papers mentioned for more complete information on analytical techniques and wind tunnel tests.

2. RSRA ROTOR LOAD-MEASUREMENT SYSTEM

Figure 3 shows the rotor load-measurement system of the RSRA compound used for hub drag measurements. The system and its calibration are described in detail in references 4 and 8; summary descriptions are given immediately below. (This system is completely different from the active isolator system originally installed on the RSRA helicopter; yet another type of load-measurement system is planned for that aircraft when it is converted to the X-Wing testbed.)

Rotor (and hub) loads are transmitted to the airframe by the seven load cells shown in figure 3. The redundant links would take up loads only if a load cell should fail; otherwise, they have no effect on load measurements.

The entire system must be calibrated when installed in the aircraft. This ensures that all measurements are traceable to the National Bureau of Standards. The reference axis system used for calibration, and for all RSRA drag data reported here, is shown in figure 4. Note that the vertical (lift, or Z) axis is aligned with the main-rotor shaft, which is tilted forward 2°. The drag-measurement (X) axis is also tilted downward 2° to align with the plane of the rotor hub. For convenient comparison to wind tunnel data, drag is defined to be positive in the aft direction, opposite to positive X; lift is defined to be positive upward, opposite to positive Z.

2.1 System Calibration

The only previous full calibration of the rotor load-measurement system used for the hub drag experiments was performed during 1980-81. The "single loads" data of that calibration (ref. 4) are the best match to the flight conditions established for the hub drag measurements. Root-mean-square (rms) system error for drag is 930 N (209 lb); for

lift, it is 300 N (68 lb). Most of the error is hysteresis. If hysteresis is assumed to be shaken out in flight by airframe vibrations, rms error drops to 200 N (46 lb) for drag and 280 N (62 lb) for lift.

(The hysteresis problem is addressed in some detail in reference 4. It is not thought to be significant for the data reported here, but it will nevertheless be carefully investigated in the forthcoming recalibration of the RSRA.)

Hub drag is much less than the full-scale rotor-calibration load of 38.3 kN (8,620 lb) in the drag axis. Full-scale rotor lift is 217 kN (48,800 lb), which is two orders of magnitude greater than maximum hub lift. Consequently, the relative measurement errors for hub loads are worse than they would be for rotor loads. Nevertheless, they are small enough for the flight tests to determine whether hub drag measurement is feasible.

Numerous improvements to the system and its calibration are possible. Some of these were implemented for the calibration of the second RSRA (ref. 9). The results of that calibration indicate that a significantly improved calibration of the RSRA compound is possible, especially in the load range appropriate for the hub drag measurements. It is now planned that a second calibration of the RSRA compound will be carried out in a manner that will allow the results to be applied to the hub drag data reported here. Accordingly, the present data should be regarded as preliminary.

2.2 Measurement Errors

Placement of the load cells between the transmission and airframe, remote from the rotor (fig. 5), allows changes to be made to the rotor without affecting the accuracy of the measurement system or requiring a new calibration. However, this arrangement also subjects the load cells to large inertial loads caused by the reaction of the transmission mass to aircraft body accelerations. These inertial loads can be readily determined and subtracted from the load cell outputs to get the true rotor hub loads. (Equations are given in ref. 4.) The instrumentation used to measure aircraft accelerations is itself subject to measurement errors; these errors, translated to equivalent rotor loads, sum to 76 N (17 lb) for drag and 9 N (2 lb) for lift. For hub load measurements, the inertial loads are a much larger source of relative error than would be the case for full-scale rotor loads.

When the RSRA is converted from one configuration to another, the net weight of the transmission, hub, and rotor (if installed) changes. Rather than attempt to recalculate all inertial effects for every configuration flown during the fixed-wing tests, tare measurements were made with the aircraft sitting still on the ground. Because lift, drag, etc. were then exactly zero, all data for each flight were easily adjusted to correct for inertial effects after taking aircraft attitude into account.

Another source of error is the onboard data system used to record load cell outputs. The rms error for drag measurements is only 9 N (2 lb), but for lift (which uses more load cells and data channels) it is 110 N (25 lb). These errors were determined in the summer of 1984,

during the fixed-wing flight tests. All other errors reported here were taken from reference 4.

A limiting source of known errors is the load application error of the calibration itself. This is the error in measuring the reference calibration load, which for drag is 76 N (17 lb), and for lift is 160 N (37 lb).

The rms sum of all known drag-measurement errors is 930 N (210 lb) including hysteresis, and 230 N (52 lb) if hysteresis is assumed to be negligible. The resulting errors for lift are nearly the same with or without hysteresis: 343 and 338 N (77 and 76 lb), respectively. Reduced errors are theoretically possible by means of the improvements suggested at the end of this paper.

An important feature of the load-measurement system is that it measures forces acting directly on the rotor hub itself. This means that it does not measure interference drag or wake effects caused by the hub. Although not a true source of error, this characteristic of the system may lead to misinterpretation of the data if not kept in mind.

It should also be mentioned that the RSRA cannot fly with the hub in a fixed position: the hub is always turning at normal transmission speed (203 rpm), even in the fixed-wing mode. Other researchers report that rotation has a slight, but detectable, effect on drag (ref. 6). For scale models, this may not be consistent with varying test conditions such as Mach number (ref. 1) and Reynolds number (ref. 10). However, Sheehy and Clark (ref. 1) report that rotation effects are negligible for unfaired hubs with a sufficient number of blade spindles. This includes the RSRA's hub (Sikorsky S-61R), which has five spindles.

Williams and Montana (ref. 11) summarize the problem with the general rule that rotation has a negligible effect if the hub advance ratio is greater than 5.0. The RSRA meets this criterion at the airspeeds tested. A rotating hub is obviously the most important flight condition. Accordingly, all data reported here were averaged over at least 15 sec of steady flight.

3. HUB DRAG AND LIFT MEASUREMENTS

3.1 Background

Rotor hub drag is a major component of total helicopter drag. A commonly accepted figure for current models is 30% (refs. 10 and 12). New helicopter fuselage designs are becoming aerodynamically cleaner through using such features as retractable landing gear, as well as paying more attention to aerodynamic detail overall. For reasonably clean, new helicopters, the rotor hub could be responsible for as much as 60% of the total drag (ref. 1). Hub drag is, therefore, becoming even more important for high speed and efficiency. New-generation hubs with elastomeric bearings have lower profiles, hence lower drag, which at least partly reduces the relative penalty. Upcoming composite and bearingless hubs promise even less drag when they reach production. The desire for ever greater speed and efficiency makes precise prediction and measurement of actual hub drag, however large or small, increasingly important.

It would seem that simply more wind tunnel tests would satisfy the requirement for better hub drag data. However, conventional wind tunnel Reynolds-number scaling and correction methods do not reliably apply to helicopter-type bluff bodies, including rotor hubs, as pointed out by such researchers as Sheehy and Clark (ref. 1) and Williams and Montana (ref. 11). Consequently, extrapolations of traditional fixed-wing wind tunnel methods to helicopter drag investigations are not always valid. Furthermore, some types of wind tunnel tests, especially investigations of hub fairings, appear to be significantly affected by scale (ref. 13).

Analytical methods are continually being improved. Sheehy and Clark (ref. 14) report agreement with wind tunnel data within $\pm 8\%$, but with $\pm 14\%$ errors for some cases. Whether numerical analysis, scale models, or full-scale wind tunnel tests are employed, it would still be prudent to verify analytical and experimental methodologies with actual flight test data to meet the demand for the highest possible accuracy and reliability.

Beyond the drag of the rotor hub itself, there is also interference drag, plus the effects of turbulent hub-wake impingement on the tail of the helicopter. In principle, the RSRA could be used to measure the gross effects of hub interference and wake impingement drag by comparing the engine power required both with and without the rotor hub, then subtracting measured hub drag. However, the accuracy of such a procedure is somewhat questionable, given the present state of development of the special flight test and analysis techniques required by the RSRA for such measurements. Accordingly, present research emphasis, including this report, is focused on the larger, immediate hurdle of determining the parasite drag of the rotor hub alone.

3.2 Wind Tunnel Tests

Several different wind tunnel tests were performed with rotor hubs representative of that used on the RSRA. Hub drag and lift measurements derived from applicable tests are plotted against angle of attack in figures 6 and 7. The original data come from three different test configurations:

(1) A full-scale S-61 rotor hub with blade shanks, mounted to a test fixture that aerodynamically simulated an S-61 upper fuselage, engine cowlings, and pylon (ref. 6). The RSRA's fuselage is closely similar, but not exactly identical, to the S-61 in this area. The major difference is a longer aft pylon ("doghouse") fairing on the RSRA; compare figure 8 with figures 1 and 9. (The RSRA's rotor hub is described in the next section, below.)

(2) The same full-scale rotor hub and test fixture, but with a "beanie" fairing on the hub (the "small fiberglass cover" mentioned in ref. 6). The beanie fairing is a flattened dome that sits on top of the hub.

(3) A 1/6-scale model of the entire RSRA (ref. 5). Again, there was no hub fairing. The model hub used there had small blade shanks and no blade folding hinges. Compared to the configurations of reference 6, it had about 0.1 m^2 (1 ft^2) less equivalent (scaled) swept frontal

area. The plotted data have been scaled up to equivalent full-scale values.

All data shown here for the two full-scale hubs were taken with the hubs rotating. The 1/6-scale hub was fixed.

(None of the models had a hub-mounted "bifilar" vibration absorber, normally flown on several versions of the Sikorsky S-61 and the RSRA, but removed for the fixed-wing flight tests.)

All data in figure 6 have been corrected to show drag in the plane of the flapping hinges, perpendicular to the rotor shaft, to be consistent with the RSRA's measurement axis system (except for a sign reversal between drag and X; see fig. 4). Figure 7 shows data for which lift is aligned with the axis of the rotor shaft and reversed in sign from Z.

The references cited typically reported data in terms of equivalent frontal area, or force divided by dynamic pressure (D/Q_∞ and L/Q_∞). Unfortunately, the available data do not allow consistent calculations of drag and lift coefficients. All data in this paper are, therefore, usually given as either forces (N) or equivalent areas (m).

The data plotted in figure 6 show a consistent slight drag increase with increasing angle of attack. The reduced frontal area of the hub on the 1/6-scale RSRA partially accounts for the large difference in hub drag for that configuration, but the full discrepancies between full-scale and small-scale average hub drag are unexplained. Note that in contrast, the 1/6-scale RSRA lift data agree well with the full-scale hub data (fig. 7).

All data plotted in figure 6 are "incremental" hub drag (that is, the differences in drag between the models with and without the hubs installed). This accordingly includes interference drag. Similarly, all data in figure 7 show the differences in lift with and without the hubs.

3.3 Flight Test Data

A series of test flights was performed with the RSRA in its fixed-wing configuration, most flights with the hub removed and two with the hub installed without blades. A major purpose of the test program was to determine fixed-wing handling qualities (ref. 2). For such tests, the hub was added to change the vertical center of gravity. Flights of the two different configurations provided an obvious opportunity to measure the drag of the rotor hub.

Figure 9 shows the RSRA flying without the rotor hub. This view was selected to show the aft pylon structure; the lateral strakes and oil cooler exhaust are clearly visible. Also visible is the circular hole needed for the pitch links normally present, with the end of the main-rotor shaft in the center. The transmission well is not sealed against airflow or pressure variations, which lead to significant values of measured drag when the hub is removed. The unsealed transmission well can also be expected to cause different aerodynamic interference

effects when the hub is installed, compared to what would be seen for a sealed pylon or a wing tunnel test of an isolated hub.

It was not possible to test the hub in a configuration that exactly matched any of the wind tunnel test hardware, for several reasons. Constraints of time and cost precluded construction of a dummy hub, and the hub actually used had to be convertible back to a fully flight-worthy hub with blades. Accordingly, the blade spindles were locked into position with a special fixture to prevent hinge damage. Figure 10 is a photograph of the hub as flown, showing the spindle lock bolted to the blade mounts; figure 11 is a cutaway side view. For reference, figure 12 shows an S-61R hub as usually flown on the RSRA.

In addition to the spindle lock, figures 10 and 11 show disk-shaped ballast weights bolted to the top of the hub. They were used to achieve the highest possible center of gravity for the handling qualities tests. The weights replaced the S-61R "beanie" fairing and bifilar assembly. (The fairing is shown in outline in fig. 11.) Compared to a standard S-61R hub, the net decrease in projected hub frontal area was 0.05 m^2 (0.5 ft^2). Compared to a bare hub, the weights increased frontal area by 0.18 m^2 (1.9 ft^2). Note that this version of the S-61 rotor hub has no blade folding hinges. Adding hinges and blade shanks would add about 0.16 m^2 (1.7 ft^2) to the swept area. All swept areas are approximate because the wind tunnel reports (refs. 5 and 6) did not give detailed dimensions from which geometrically equivalent areas could be accurately calculated.

Dynamic pressure was always measured by the nose boom so that it could be corrected to dynamic pressure at infinity. This allows direct comparison to wind tunnel data, but does not necessarily equal dynamic pressure at the hub itself.

Figures 13-18 show data collected at several different airspeeds, with and without the hub. Figure 13 shows the basic drag force data plotted against airspeed; figure 14 shows lift. The same data are replotted in figures 15 and 16, converted to equivalent flat-plate drag and lift area (force divided by dynamic pressure) and plotted against dynamic pressure. If there were no angle-of-attack effects, the data would ideally fall into two straight, horizontal lines. Figures 17 and 18 show the same data, plotted this time against fuselage angle of attack.

Scales for all pairs of figures are the same magnitude for lift and drag, but the vertical axes for lift data are slightly offset to better show the data points near zero. All lift data were adjusted to eliminate tare effects, as described above in the section entitled "Measurement Errors."

The net drag and net lift are the differences between the hub-on data and the hub-off data. In flight tests, it was usually not possible to exactly match airspeed or angle of attack between different flights (unlike the wind tunnel test data shown in figs. 6 and 7). To determine net hub forces, it was consequently necessary to perform separate curve fits to all hub-on and hub-off data, and then to subtract predicted forces for the hub-off data from the hub-on predictions.

The resulting estimates of net hub drag and lift are plotted as straight lines in figures 13-18. The solid parts of the lines cover ranges of overlap between hub-on and hub-off data. (The different weights and drags between the two configurations prevented exact overlap: the RSRA was slower and heavier with the hub installed than without the hub, and had to fly at a higher angle of attack at any given airspeed.) In principle, the predicted drag and lift lines in figures 13 and 14 should be parabolic (second-order polynomials), and should intersect the axes at zero load and airspeed. However, a straight-line fit is adequate for the speed range shown. A slight second-order nonlinearity is visible in the hub-on data in figure 17, but it is hardly greater than the data scatter; therefore, a straight-line fit is also sufficient here.

Figures 19 and 20 show completely different drag and lift data. The data were taken at the same airspeed, hence the same dynamic pressure, for each flight, and were plotted against fuselage angle of attack. For these data, angle of attack was varied by changing the angle of incidence of the wing. The RSRA automatically retrims to maintain a constant wing angle of attack, hence nearly constant lift, airspeed, and altitude. The net effect is that the wing stays fixed while the fuselage rotates around it (ref. 3). This unique capability of the RSRA allows angle-of-attack variations to be performed at constant airspeed, thus providing significantly cleaner data than is normally possible. It should be noted that fuselage and wing angles of attack are measured independently, with separate air data booms, on the RSRA.

For consistent comparison to figures 15-18, the data in figures 19 and 20 were converted to equivalent flat-plate areas. The total ranges of the constant Q data are shown as vertical bars in figures 15 and 16. Since the dynamic pressure was constant, the raw data were merely scaled by a constant to get the data points plotted in figures 19 and 20. Accordingly, there are no separate plots corresponding to figures 13 and 14.

The data for figures 19 and 20 were taken at 85 m/sec (166 knots) calibrated airspeed for a dynamic pressure of 4.4 kN/m^2 (92 lb/ft^2). The resulting equivalent drag-measurement error is 0.053 m^2 (0.57 ft^2); the lift error is 0.077 m^2 (0.83 ft^2). These equivalent errors are approximately correct for the data in figures 13-18.

Both drag and lift data for figures 19 and 20 show obvious nonlinear behavior. Accordingly, second-order polynomial curve fits were used to derive net force predictions. Note that these curve in the opposite direction from the raw data. For figures 19 and 20, the total changes in drag and lift over the angle-of-attack range are hardly greater than the measurement accuracies. Consequently, it is possible that the nonlinear curve fits of figures 19 and 20 are artifacts resulting from the small number of data points. For the drag data (fig. 19), however, the shape of the net drag curve is similar to those shown by Churchill and Harrington (ref. 15).

The wind tunnel data (shown in figs. 6 and 7) reveal little more variation with angle of attack than the flight data reveal. The flight data are consistent with the results reported in references 13 and 15,

which show relatively minor drag variations of less than 0.1 m^2 (1 ft^2). This result supports the obvious conjecture that the airflow follows the top of the pylon, reducing the total angle-of-attack change seen locally by the hub. The drag data for the 1/6-scale RSRA model do show a large percentage of change, but the angle of attack range is much greater for the model than for the flight data.

The RSRA's rotor shaft is inclined 2° forward of true vertical, and the pylon immediately below it is sloped forward with respect to the horizontal, as is visible in figure 1. The shaft hole also slopes forward, so that airflow into it would be expected to increase slightly as the fuselage angle of attack decreases. The trends in the gross drag data in figure 19 are consistent with this hypothesis, but other aerodynamic interference effects cannot be discounted using the existing data.

3.4 Summary Data

Table 1 gives numerical data for net drag and lift for different test configurations. Average values for the data in figures 15 and 16 are given first. All other values are given for a specified fuselage angle of attack (α), usually 0° for convenience. For the flight test data, the values were predicted by the regressions used to determine the lines of net drag and lift plotted in figures 17-20. The 1/6-scale wind tunnel tests had data points at exactly 0° , but the most appropriate points for the full-scale wind tunnel tests were at $+2^\circ$. This is because the full-scale models had 4° shaft tilts, instead of the 2° tilt on the actual RSRA and the 1/6-scale model.

When considering the data in table 1, the following cautions should be kept in mind. (1) The hub configurations are not identical. In particular, the model hubs do not include spindle locks or ballast weights. (2) The RSRA measures hub drag and lift directly with its load cell system, but the wind tunnel models measure "incremental" drag and lift. Interference effects on the fuselage are not directly measured by the RSRA in flight, as they would be in a wind tunnel. (3) The existing calibration of the RSRA load cell system was not optimized for low load levels, hence the calibration corrections cannot be exactly matched to the loads actually measured.

In table 1, the discrepancies between different values of lift and drag measured in flight are less than the equivalent measurement errors given above. If one considers the 0.18-m^2 (1.9-ft^2) increase in swept area of the hub as flown, compared to the hub as tested on the 1/6-scale RSRA (ref. 6), then the differences in measured hub drag are also small. For all other wind tunnel data, the differences in measured drag cannot be explained by differences in swept area.

No explanations are available for the differences in measured lift between flight and wind tunnel data. Even agreement between different wind tunnel data is suspect: the 1/6-scale RSRA value should match the full-scale bare-hub data, not the data for the full-scale hub with "beanie" fairing. Note that the pylon shape of the 1/6-scale RSRA model is the same as the actual aircraft, so different local flow patterns cannot explain the change in sign of measured lift between flight and wind tunnel data.

Recasting the flight test results given in table 1, the rotor hub drag coefficient ranges from 0.73 to 0.79, based on a projected (swept) frontal area of 0.61 m^2 (6.6 ft^2). These numbers lie barely within or slightly beyond the range of 0.5 to 0.76 reported by Churchill and Harrington (ref. 15). Also, the larger value fits almost exactly the drag coefficient predicted by equation (1) in reference 14, but this is probably fortuitous.

4. PROPOSED IMPROVEMENTS

As with any flight test program, numerous compromises had to be made for the sake of safety and efficiency. Now that the RSRA has been successfully flown in its fixed-wing configuration, and the ability to measure rotor hub drag has been demonstrated, more refined and extensive experiments can be confidently proposed. Several possible improvements to the RSRA's systems and test techniques are discussed below.

The most obvious improvement--flight test of a hub more representative of a standard S-61R configuration--is perhaps the most difficult because of airworthiness requirements. When the blades are removed, the spindles must be locked to prevent damage to the hinges. The spindle lock structure (figs. 10 and 11) precludes installation of the normal S-61R "beanie" fairing or bifilar assembly, although the lock could be modified to accept the beanie fairing. A special hub with dummy spindles and hinges would have to be made in order to test the complete standard configuration. Such a test could then be extended to include blade shanks, if desired. Similar considerations may apply to other hubs chosen for flight test, depending upon the details of their designs.

For all fixed-wing flights flown to date, safety considerations favored reducing the total range of wing incidence variations to $\pm 5^\circ$. The range of incidence can be more than doubled to $\pm 12^\circ$ (-9° to $+15^\circ$), providing a useful increase in obtainable data. Also, local angle of attack and dynamic pressure could be measured immediately in front of the hub with a pylon-mounted probe. If necessary, the effects of local angle of attack and dynamic pressure could be further explored by replacing the hub with a reference object (a sphere or flat disk) with known lift and drag characteristics. This would also provide a limited in-flight check calibration of the load-measurement system.

Another improvement would be more careful determination of interference effects between the hub, the pylon, and the shaft hole. With the pitch links removed, a temporary fairing could greatly reduce the size of the hole, leaving only the end of the rotor shaft exposed to allow measurement of true shaft drag. Covering the shaft with a well-sealed fairing would then permit the best possible determination of zero-drag measurement tares. Although small, such tares can have an important effect of measurement on interference drag, which can be quite small compared to the total drag. In principle, interference effects could be further examined by changing the separation between the hub and pylon with rotor shaft extensions. However, this is best done by wind tunnel tests, using flight tests only to verify critical configurations.

Large-scale interference effects can be examined by measuring the effects of the hub on total fuselage drag. The RSRA has the potential of measuring wing drag and auxiliary engine thrust, which would help to isolate the effects of the fuselage and hub. Such tests would preferably be done in conjunction with tests of a sealed shaft hole. The engine thrust-measurement system was not usable during the fixed-wing flight program; at present, thrust must be derived from engine performance data. For future programs, the thrust-measurement system must be modified and calibrated to obtain full accuracy. The wing load-measurement system was used for all flights, but it requires calibration to verify its performance. It is planned to reanalyze all wing load data when wing calibration is complete, and then to deduce fuselage drag and lift effects.

An important area of improvement lies in ground tests needed to support the flight test program. The need to calibrate the wing and auxiliary-engine load-measurement systems has already been mentioned; however, recalibration of the rotor load-measurement system has, in fact, higher priority. The major reason is that the previous calibration (ref. 4) showed disproportionate error near zero load, which unfortunately is exactly the same load range in which the hub drag data fall. However, improved calibration equipment and procedures have led to increased calibration accuracy in the low load range, as demonstrated during the calibration of the second RSRA (ref. 9). Recalibration of the RSRA compound version can be confidently expected to result in improved load-measurement accuracy near zero load. Also, it is a simple matter to acquire extra calibration data at low loads, so that analytical results can be better matched to the hub load range. Any improvements in usable accuracy will be applicable to data already acquired, provided that no modifications have been made to the aircraft itself in the meantime.

Mechanical improvements to the RSRA's load-measurement systems are also possible. Installation of elastomeric bearings in the load cell mounts should greatly reduce hysteresis, increasing accuracy over the entire load range. However, such a modification would necessitate yet another calibration, and would not help improve the analysis of existing data.

5. CONCLUSIONS AND RECOMMENDATIONS

Rotor hub drag and lift were successfully measured in flight using the RSRA's rotor load-measurement system. Although the hub used did not exactly match any standard configuration, the RSRA's ability to make drag and lift measurements comparable to wind tunnel data was demonstrated to be adequate.

Recommendations for future testing include replacing the hub weights with a standard fairing (near term) and using a dummy hub without a spindle lock (longer term) to better match existing wind tunnel data. More extensive flight data over a greater angle-of-attack range would be helpful. The RSRA rotor load-measurement system should be recalibrated for better data analysis.

REFERENCES

1. Sheehy, T. W.; and Clark, D. R.: A General Review of Helicopter Hub Drag Data. Paper presented at the 31st Annual National Forum of the American Helicopter Society, Washington, D.C., May 1975. Also published in the Journal of the American Helicopter Society, vol. 22, no. 2, Apr. 1977.
2. Painter, W. D.; and Erickson, R. E.: Rotor Systems Research Aircraft Airplane Configuration Flight-Test Results. Paper presented at the AIAA/AHS/ASEE Aircraft Design, Systems and Operations Meeting, San Diego, Calif., Oct. 31-Nov. 2, 1984.
3. Hall, G. W.; and Morris, P. M.: Flight Testing the Fixed Wing Configuration of the Rotor Systems Research Aircraft. Paper presented at the 28th Symposium of the Society of Experimental Test Pilots, Beverly Hills, Calif., Sept. 26-29, 1984.
4. Acree, C. W.: Results of the First Complete Static Calibration of the RSRA Rotor Loads Measurement System. NASA TP-2327, Aug. 1984.
5. Flemming, R.; and Ruddell, A.: RSRA Sixth Scale Wind Tunnel Test Final Report. SER-72011, Sikorsky Aircraft, Division of United Aircraft Corporation, Stratford, Conn., 1974.
6. Olson, J. R.: Wind Tunnel Data and Analysis of Full Scale Rotor Head and Pylon Drag Investigation. SER-61027, Sikorsky Aircraft, Division of United Technologies Corporation, Stratford, Conn., 1960.
7. Rotorcraft Parasite Drag. Presented to the 31st Annual National Forum of the American Helicopter Society, special report by the Ad Hoc Committee on Rotorcraft Drag, Washington, D.C., May 1975.
8. Acree, C. W.; et al.: RSRA Static Calibration Facility Operations Manual. NASA TM-84389, Aug. 1983.
9. Acree, C. W.: Verification of Static Rotor-Load Measurement Capabilities of the RSRA Helicopter Active-Isolator System. Paper presented at the AHS National Specialists' Meeting on Helicopter Testing Technology, Williamsburg, Va., Oct. 29-Nov. 1, 1984.
10. Keys, C. N.; and Rosenstein, H. J.: Summary of Rotor Hub Drag Data. NASA CR-152080, Mar. 1978.
11. Williams, R. M.; and Montana, P. S.: A Comprehensive Plan for Helicopter Drag Reduction. Paper presented at the 31st Annual National Forum of the American Helicopter Society, Drag Committee Report, Washington, D.C., May 1975.
12. Gormont, R. E.: Some Important Practical Design Constraints Affecting Drag Reduction. Paper presented at the 31st Annual National Forum of the American Helicopter Society, Drag Committee Report, Washington, D.C., May 1975.

13. Logan, A. H.; Prouty, R. W.; and Clark, D. R.: Wind Tunnel Tests of Large- and Small-Scale Rotor Hubs and Pylons. USAAVRADCOM Technical Report 80-D-21, 1981.
14. Sheehy, T. W.; and Clark, D. R.: A Method of Predicting Helicopter Hub Drag. USAAMRDL Technical Report 75-48, Ft. Eustis, Va., 1976.
15. Churchill, G. B.; and Harrington, R. D.: Parasite-Drag Measurements of Five Helicopter Rotor Hubs. NASA MEMO 1-31-59L, Feb. 1959.

TABLE 1.- HUB DRAG AND LIFT FOR VARIOUS TEST CONFIGURATIONS

	Drag area, m ² (ft ²)	Lift area, m ² (ft ²)
Flight test, average ^a	0.48 (5.2)	0.32 (3.5)
Flight test, $\alpha = 0^\circ$.48 (5.2)	.31 (3.3)
Flight test, $\alpha = 0^\circ$ (constant Q) ^b	.44 (4.8)	.24 (2.6)
1/6-scale RSRA, ^c $\alpha = 0^\circ$.34 (3.6)	-.10 (-1.0)
Full-scale hub, ^d with "beanie," $\alpha = +2^\circ$.91 (9.8)	-.13 (-1.4)
Full-scale hub, ^d unfaired, $\alpha = +2^\circ$.95 (10.2)	-.24 (-2.6)

^a80-115 m/sec (150-220 knots); $Q = 3.6-7.9 \text{ kN/m}^2$ (75-165 lb/ft²).

^b85 m/sec (166 knots); $Q = 4.4 \text{ kN/m}^2$ (92 lb/ft²).

^cReference 5.

^dReference 6.

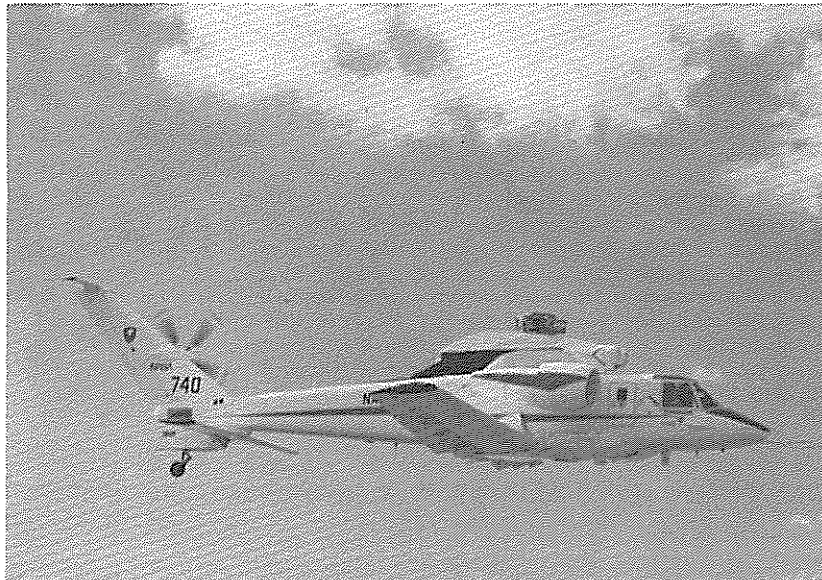


Figure 1.- RSRA fixed-wing configuration, with the rotor hub, in flight.

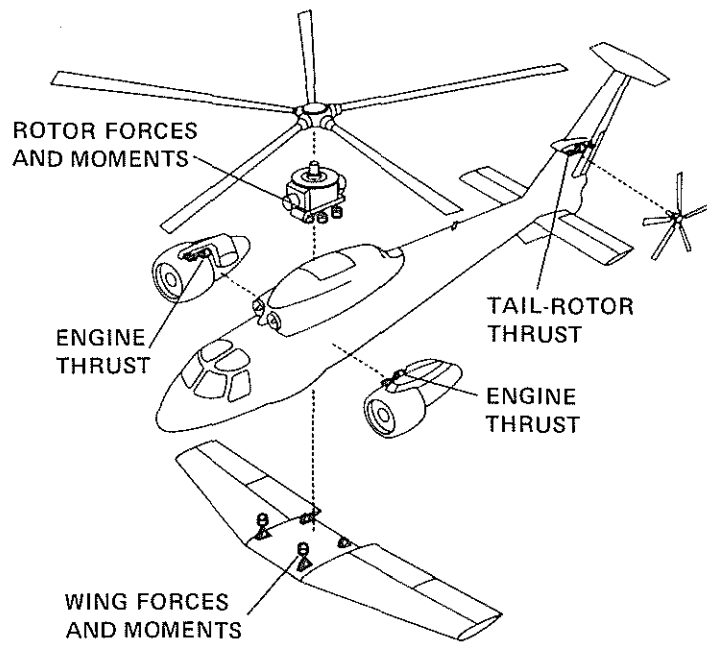


Figure 2.- RSRA load-measurement systems.

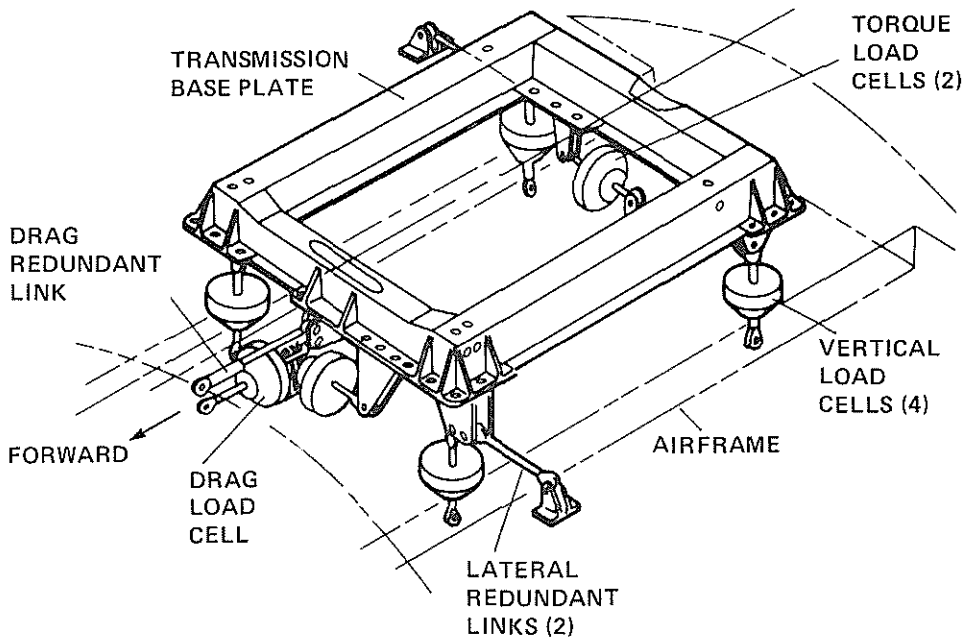


Figure 3.- RSRA rotor load-measurement system.

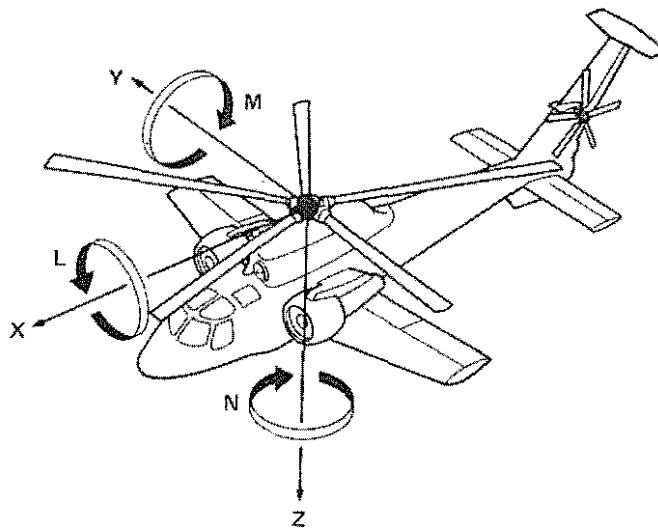


Figure 4.- Rotor and hub measurement axes.

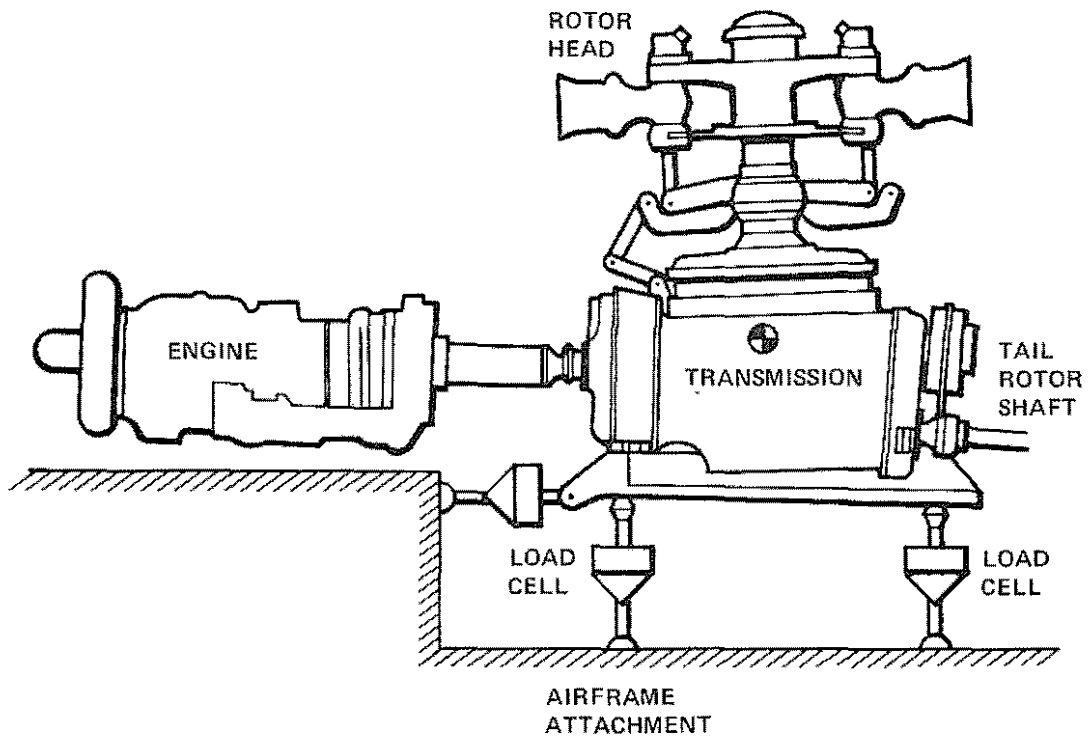


Figure 5.- Side view of RSRA transmission and load cell mounting.

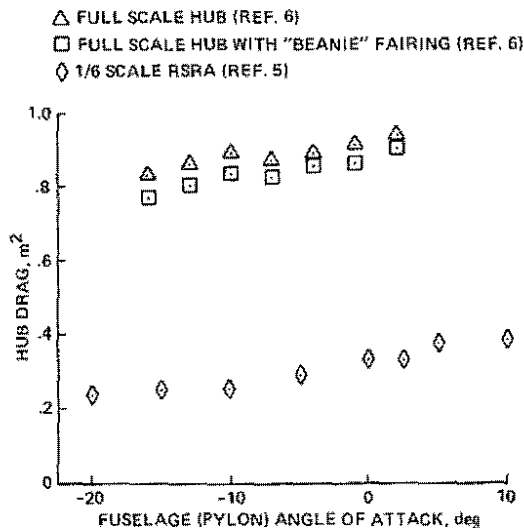


Figure 6.- Wind tunnel measurements of hub drag.

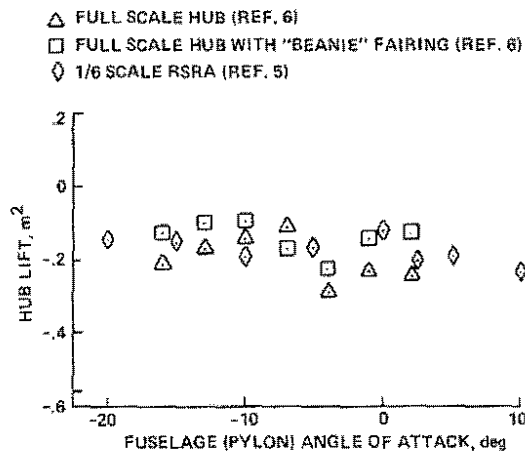


Figure 7.- Wind tunnel measurements of hub lift.

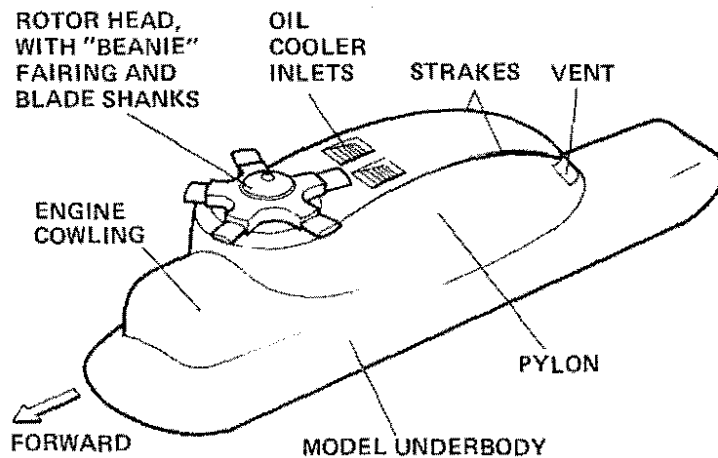


Figure 8.- Full-scale hub and pylon wind tunnel model (from ref. 6).

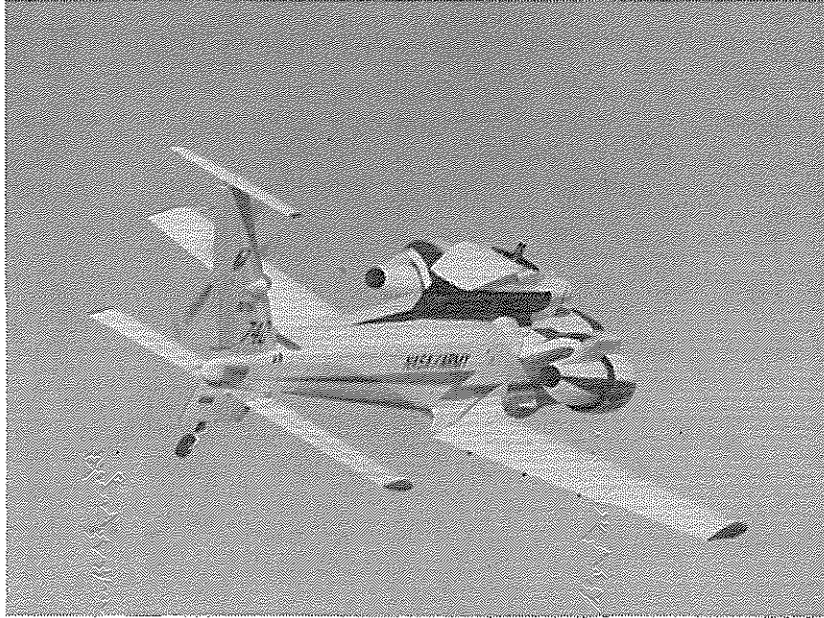


Figure 9.- RSRA in flight without the rotor hub.

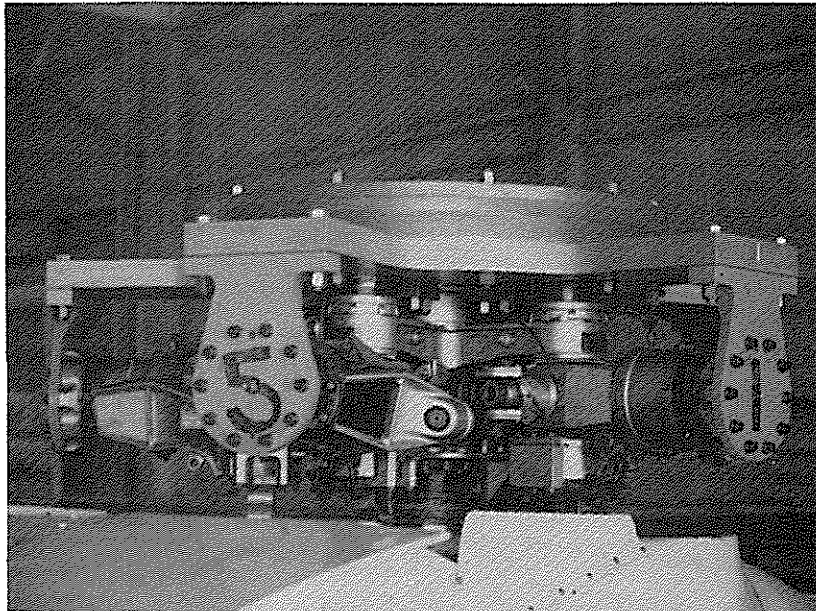


Figure 10.- RSRA rotor hub, with spindle lock and ballast weights.

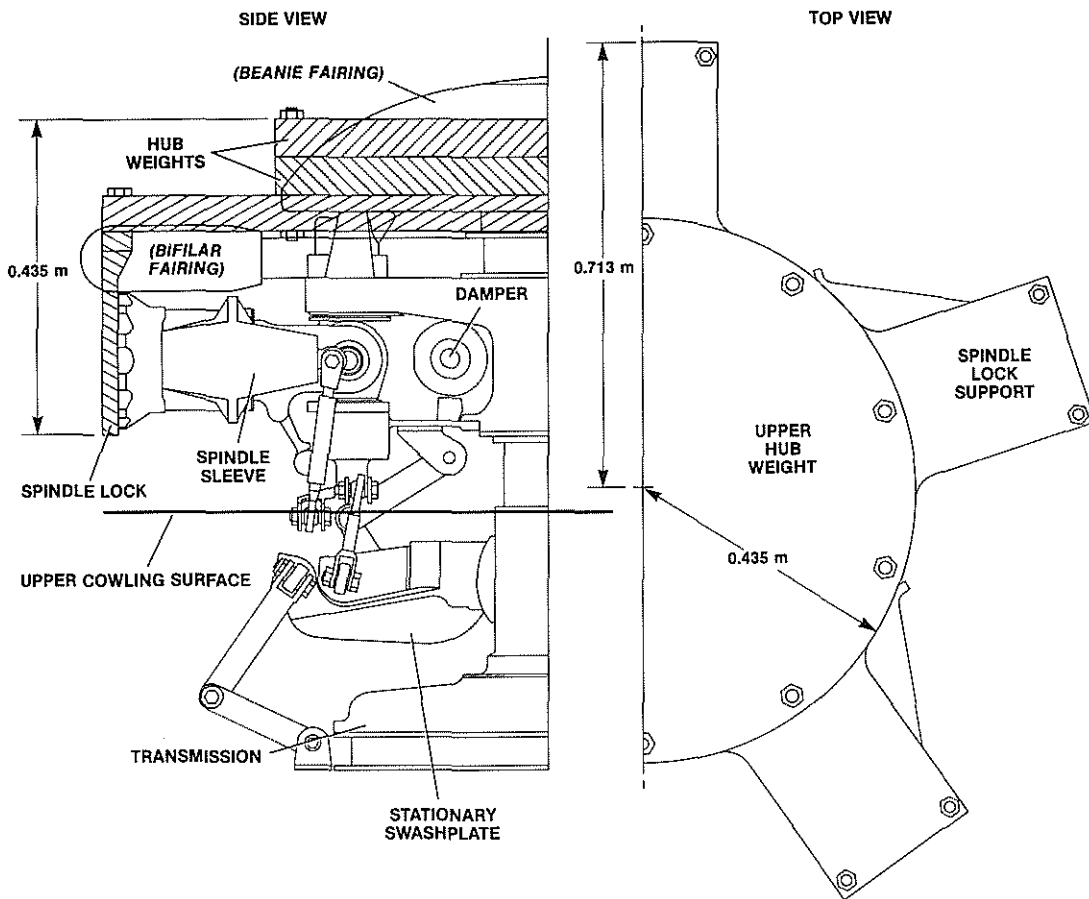


Figure 11.- RSRA rotor hub, with spindle lock and ballast weights.

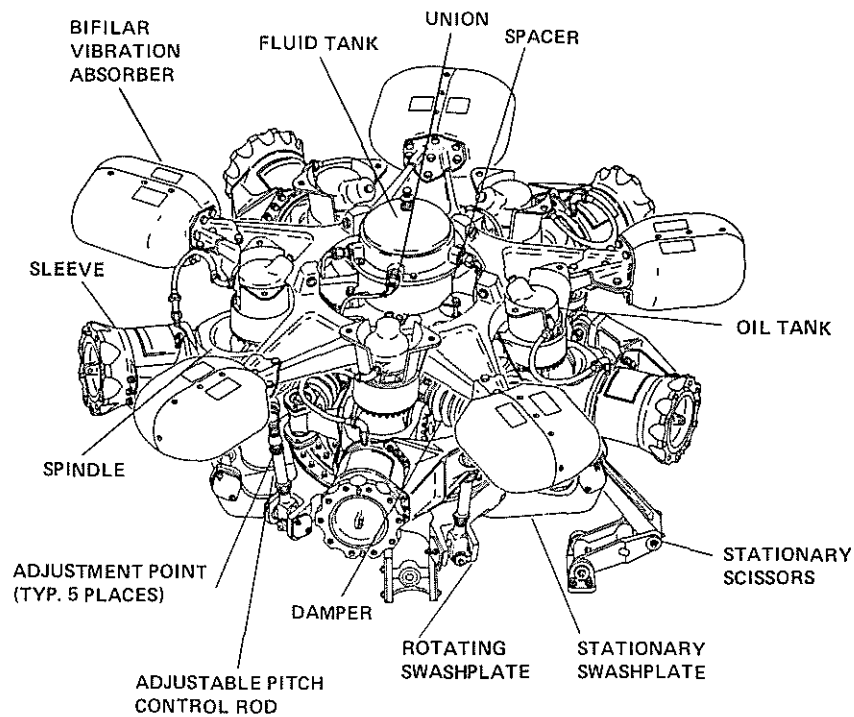


Figure 12.- Standard configuration of RSRA rotor hub. (The "beanie" fairing has been deleted to reveal detail.)

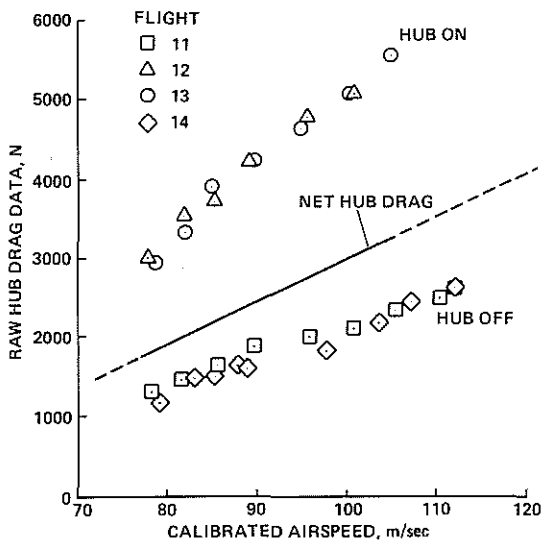


Figure 13.- Measured hub drag versus airspeed.

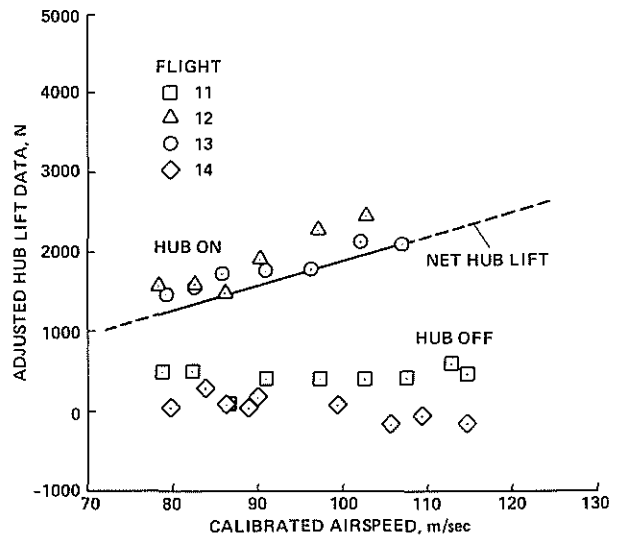


Figure 14.- Measured hub lift versus airspeed.

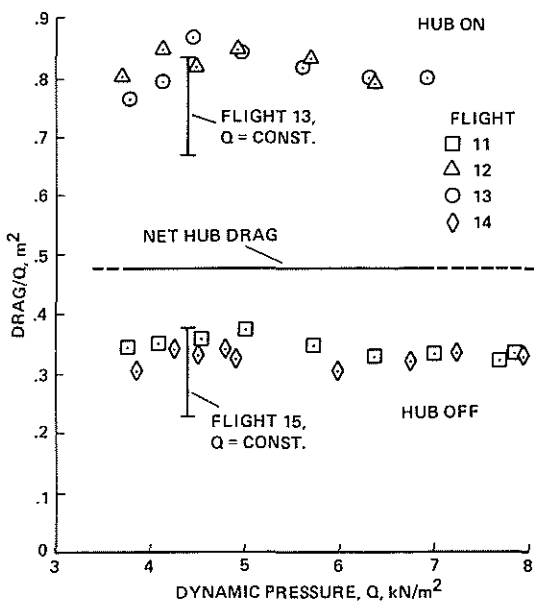


Figure 15.- Normalized hub drag versus dynamic pressure.

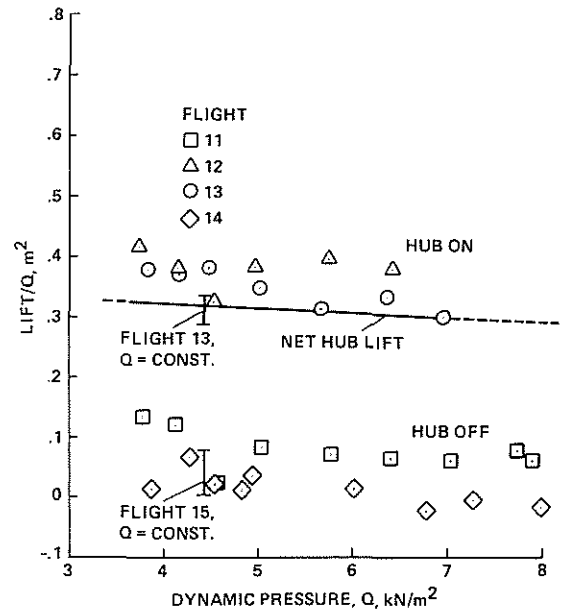


Figure 16.- Normalized hub lift versus dynamic pressure.

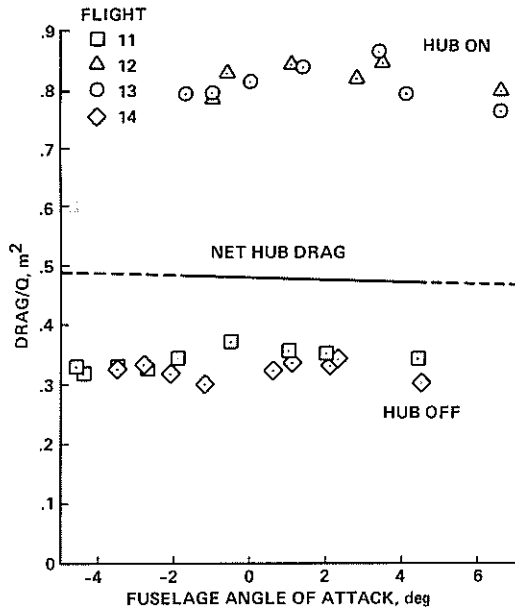


Figure 17.- Normalized hub drag versus angle of attack.

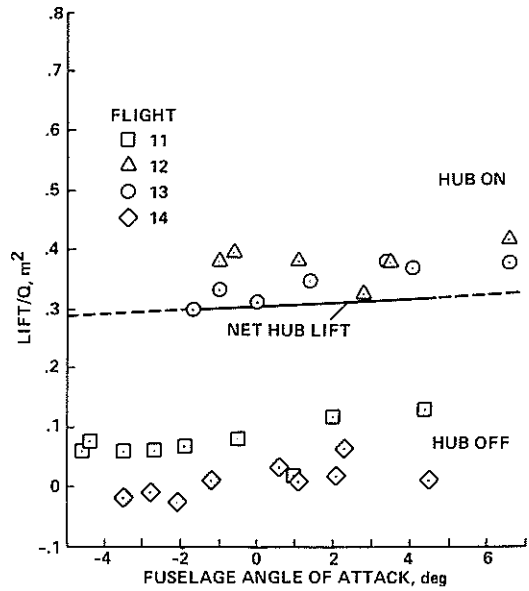


Figure 18.- Normalized hub lift versus angle of attack.

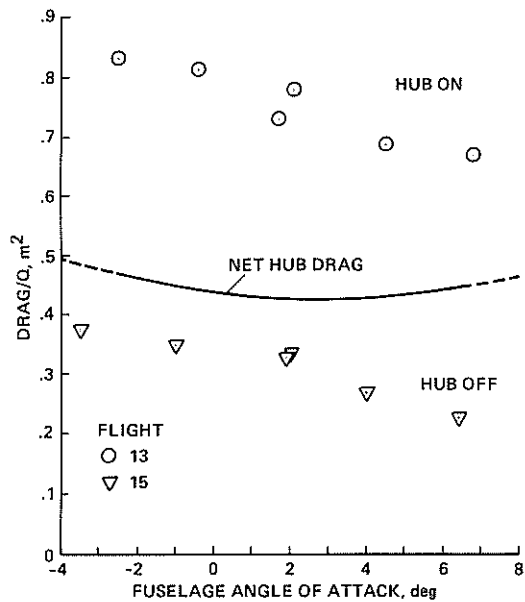


Figure 19.- Normalized hub drag versus angle of attack at constant dynamic pressure ($= 4.4 \text{ kN/m}^2$).

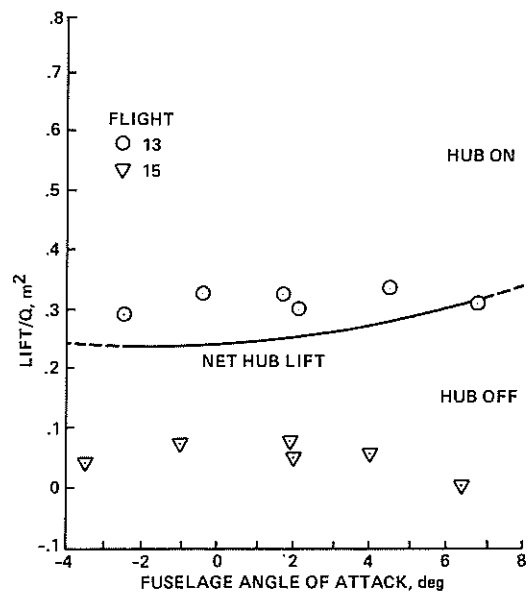


Figure 20.- Normalized hub lift versus angle of attack at constant dynamic pressure ($= 4.4 \text{ kN/m}^2$).